Petroleum Science 23 (2026) 3710–3720

Contents lists available at ScienceDirect

Petroleum Science

journal homepage: www.keaipublishing.com/en/journals/petroleum-science

Original Paper

Miscibility enhancing agents for improving oil recovery of CO_2 flooding in low-permeability reservoirs: A study based on core displacement and nuclear magnetic resonance

Chuan-Jie Ren [a,1], Yong-Liang Yang [b,1], Hong-Jun Zhang [c], Dao-Yi Zhu [b,*]

[a] Institute of Energy, Peking University, Beijing, 100871, China
[b] School of Petroleum, China University of Petroleum-Beijing at Karamay, Karamay, 834000, Xinjiang, China
[c] School of Chemical Engineering and Technology, Tianjin University, Tianjin, 300072, China

ARTICLE INFO

Article history:
Received 19 January 2026
Received in revised form
19 March 2026
Accepted 8 April 2026
Available online 13 April 2026

Edited by Min Li

Keywords:
CO_2 miscible flooding
Miscibility enhancing agent (MEA)
Core displacement
Nuclear magnetic resonance (NMR)
Minimum miscible pressure (MMP)

ABSTRACT

CO_2 miscible flooding is a key method to improve oil recovery. However, under most petroleum reservoir conditions, CO_2 cannot achieve miscibility with crude oil. Therefore, reducing the minimum miscible pressure (MMP) between CO_2 and crude oil has become a critical objective. This study investigated MMP reduction and CO_2 displacement efficiency of miscibility-enhancing agent (MEA) using low-permeability artificial cores and reservoir oil samples from the Xinjiang Oilfield. A core displacement method was established to determine the MMP and, in parallel, to screen four candidate MEAs. Nuclear magnetic resonance (NMR) technology was employed to probe the pore-scale mechanisms by which MEAs reduce the MMP between crude oil and CO_2. Results showed that, before adding an MEA, the baseline MMP of CO_2–crude oil system was 21.38 MPa. Among the four MEAs, tributyl citrate (TC) exhibited the strongest effect, lowering the MMP by 1.61 MPa. TC concurrently improved CO_2 conformance efficiency in both large pores and small pores, improving oil recovery during CO_2 flooding. These results demonstrated that TC-enabled miscibility tuning offers a practical pathway to reduce MMP and improve CO_2 conformance in low-permeability reservoirs. It provided a foundation for pilot-scale conformance control implementation in the Xinjiang Oilfield and analogous CO_2 flooding reservoirs.

1. Introduction

Low-permeability petroleum reservoirs have small pore structures, fine flow channels, and strong capillary confinement. Conventional waterflooding and gas flooding cannot achieve effective development, and oil recovery enhancement faces significant bottlenecks (Bai et al., 2025; Zhu et al., 2026). CO_2 miscible flooding can reduce oil–gas interfacial tension, cause swelling, and extract intermediate fractions. Therefore, it significantly lowers residual oil saturation, decreases mobility ratio and improves CO_2 conformance performance, and is an important technical approach to improve oil recovery in low-permeability reservoirs (Fu et al., 2024; Gandomkar et al., 2025; Wang et al., 2023; Zhu, 2025). For low-permeability and tight reservoirs, developing CO_2 miscible or near-miscible technologies adapted to reservoir temperature and pressure and crude oil composition is of important engineering significance and economic value (Zhu, 2022).

Although CO_2 miscible flooding has clear mechanistic advantages, many low-permeability reservoirs have heavier crude oil components, higher polarity, and higher contents of resins and asphaltenes. These factors make it difficult for CO_2 and crude oil to achieve totally miscibility under reservoir conditions (Cao and Gu, 2013b; Sennaoui et al., 2022; Wang and Gu, 2011). The minimum miscible pressure (MMP) is generally higher than the attainable reservoir pressure, and actual reservoir development often stays in non-miscible or near-miscible states (Cao and Gu, 2013a; Luo et al., 2024). Therefore, it is necessary to add miscibility enhancing agents (MEA) to regulate phase behavior and interfacial properties.

* Corresponding author.
E-mail address: chutaoi@163.com (D.-Y. Zhu).
Peer review under the responsibility of China University of Petroleum (Beijing).
[1] Co-first author (both authors contributed equally to this work).

https://doi.org/10.1016/j.petsci.2026.04.011

MEA can reduce MMP, improves mobility ratio, and delays gas channeling. It achieves higher oil recovery under near-miscible or miscible conditions (Almobarak et al., 2021; Li et al., 2024). Compared with simply increasing injection pressure or changing process parameters, MEA matches crude oil composition and reservoir characteristics through flexible chemical means. (Guan et al., 2025; Guo et al., 2017). Therefore, screening MEA and elucidating mechanisms has significant research value and urgent engineering demand.

Centered on lowering the CO_2–crude oil minimum miscible pressure (MMP) and improving oil recovery under near-miscible conditions, academia and industry explore multiple types of miscibility enhancing agents (MEA) (Al-Hakami et al., 2025a, 2025b; Kuang et al., 2021; Liu et al., 2019; Sarbu et al., 2000; Wang et al., 2024; Yang et al., 2019; Zhao et al., 2025a). First, fluorinated MEAs, such as fluorinated surfactants and fluorinated ether/fluorinated compound co-solvents, have CO_2 affinity and tunable hydrophobic and oleophobic properties. They form stable micro-aggregates and diffusion layers in the CO_2 phase, effectively lowering interfacial tension, and improving mutual solubility (Costa Gomes and Pádua, 2003; Du et al., 2009; Eastoe et al., 2003). However, they face constraints of higher cost and the need for prudent evaluation of reservoir compatibility (Enick et al., 1998; Song et al., 2025).

Second, peracetylated glucose ester MEAs have multiple functional groups and strong polarity. They can form a degree of co-solubility with CO_2 and interact with middle distillates, aromatic, and polar components in crude oil. They help break interfacial films and lower MMP (Zhou et al., 2022). Their potential lies in relatively broad sources and designable molecular structures, but their adsorption and transport behavior in high-salinity and high-wax reservoirs require systematic evaluation (Song et al., 2024).

Third, multi-branched ester MEAs have strong hydrogen-bonding action, with representative molecules containing multiple carboxylic ester groups and hydroxyl sites. They interact with polar components in crude oil (such as resins and asphaltenes) through hydrogen bonding and dipole interactions. They disrupt stable interfacial film structures and lower oil–gas interfacial tension and capillary forces (Voon and Awang, 2014). They also serve as co-solvents in the CO_2 phase. They can improve CO_2 swelling and extraction of medium-to-heavy components under near-miscible regimes (Almobarak et al., 2021). Zhao et al. (2025b) used molecular simulation and core displacement to compare several MEAs (triisobutyl citrate, butyl benzoate, and ethylene glycol butyl ether). They found that triisobutyl citrate reduces the CO_2–oil interfacial tension by lowering crude oil viscosity and enhancing CO_2 extraction capability. Core experiments showed that injecting 0.07 PV triisobutyl citrate as a preflush slug increases CO_2 displacement recovery from 47.8% to 59.9%. Zhao et al. (2021) compared two MEAs, citric acid isobutyl ester and citric acid isopentyl ester. At an injection of 0.003 PV, MMP decreased by 20.61% (i.e., 6.1 MPa) and 18.58% (i.e., 5.5 MPa), respectively, and the former achieved 6.5–11.6 percentage points higher oil recovery. Liu et al., 2025 compared ether surfactants (i.e., fatty alcohol polyoxyethylene ether and fatty alcohol polyoxypropylene ether) and ester surfactants (i.e., tri-n-butyl citrate and triacetin) for MMP reduction. For ether surfactant additives, increasing the degree of polymerization (CO_2-philic groups) weakens the MMP-lowering effect. Oxygen atoms in functional groups contribute more to increasing miscibility than carbon atoms. Among ester surfactants, triacetin produces the best MMP reduction (i.e., an 11.82% decrease at 3.0 wt%), which is attributed to its symmetric short side-chain structure and ester groups. Notably, its use concentration was as high as 3.0%, and no core displacement experiments were conducted to verify recovery (Gao et al., 2010). Therefore, previous studies and field trials showed that different types of MEAs achieved certain effects in increasing oil recovery and delaying gas channeling.

In this study, we conducted systematic research on lowering MMP and improving oil recovery during CO_2 flooding in low-permeability reservoirs. A core-displacement-based method was established for MMP determination and MEA screening. The method was characterized by a short testing period and high reliability. We screened and compared four MEAs, such as petroleum ether (PE), Tween 80, tri-n-butyl citrate (TC), and lauryl alcohol polyether-4 (LAP-4), for oil recovery improvement and gas conformance control. Under controlled pressure, slug size, and formulation, we evaluated oil recovery increases, gas channeling delay, and the pressure difference response between the two ends. This can help understanding of the mechanism of action of the MEA at the core scale. NMR was also used to resolve T_2 signal (i.e., oil saturation) changes in large and small pores. The study elucidated how multi-branched esters (i.e., TC) reduced the CO_2 displacement MMP and increased miscibility. The results provided a replicable evaluation framework and optimized formulations for CO_2 (near-)miscible displacement development in low-permeability reservoirs.

2. Experimental materials and methods

2.1. Experimental materials

Potassium chloride (KCl), sodium chloride (NaCl), calcium chloride ($CaCl_2$), magnesium chloride hexahydrate ($MgCl_2{\cdot}6H_2O$), sodium sulfate (Na_2SO_4), and sodium bicarbonate ($NaHCO_3$) were analytical grade. Lauryl alcohol polyether-4 (LAP-4), petroleum ether (PE, boiling range 60–90 °C), Tween 80, and tri-n-butyl citrate (TC) were used, as shown in Fig. 1. These reagents were purchased from Shanghai Macklin Biochemical Co., Ltd. High-purity CO_2 (analytical grade, 99.9%) was purchased from Karamay Zhongke Gas Co., Ltd. Deionized water had a resistivity of 18.2 MΩ cm. The simulated formation water formulation was shown in Table 1. The water type was $NaHCO_3$-type. The total salinity was 12,932 mg/L.

The crude oil (density at 80 °C in the reservoir of 0.733 g/cm^3, viscosity 2.9 mPa·s, wax content 5.5%, pour point 16.8 °C) was taken from Zone 530 of the Xinjiang Oilfield, China. The experimental core samples were synthetic conglomerate core samples. The gravel content was 10%, and the quartz sand content was 90%. The cylindrical cores had a diameter of 2.5 cm and a length of 7 cm. The gas-measured permeability was around 50×10^{-3} μm^2. The detailed specifications were shown in Table 2.

2.2. Core-displacement method to determine the MMP of CO_2 flooding

Core-displacement method to determine the MMP of CO_2 flooding was as followed.

(1) The constant-temperature oven was set to the reservoir temperature of 80 °C. After reaching 80 °C, the temperature was stabilized for at least 2 h. The dried core was placed in

Table 1
Ion composition of simulated formation water.

Ion composition	CO_3^{2-}	HCO_3^-	SO_4^{2-}	Cl^-	Mg^{2+}	Ca^{2+}	Na^+&K^+
Concentration, mg/L	538	756	73	6594	170	15	4786

Table 2
Parameters of synthetic core samples for oil-displacement experiments.

Core No.	Length, cm	Diameter, cm	Water-measured permeability, $\times 10^{-3}$ μm^2	Porosity, %
50-15	7.060	2.531	35.18	15.81
50-13	7.064	2.531	39.02	14.35
50-7	7.069	2.534	46.75	14.31
50-16	7.065	2.532	33.42	14.84
50-11	7.057	2.530	37.75	14.76
50-25	7.062	2.521	44.68	9.94
50-37	7.052	2.502	29.51	10.67
50-29	7.033	2.520	42.32	10.02
50-21	7.042	2.521	39.47	10.16
50-27	7.078	2.518	44.89	9.57
50-38	7.055	2.502	30.28	10.36

the core holder. A vacuum pump was connected, and a vacuum was applied for at least 8 h.

(2) Formation water was prepared. Required inorganic salts were weighed and added to deionized water with stirring until being dissolved.

(3) After evacuation, the core was saturated with formation water using the ISCO pump. A constant injection pressure of 6 MPa was maintained until the pressure no longer changed. The volume of injected synthetic formation water was recorded to determine pore volume (PV) and porosity.

(4) The experimental apparatus was connected as shown in Fig. 2, and the leak-tightness of the system was checked. Reservoir crude oil was injected with an ISCO pump at a constant rate of 0.1 mL/min. Injection was stopped when no more water was produced at the outlet of the core holder, completing oil saturation of the core. The volume of produced water during oil saturation was recorded as the saturation volume, and then the initial oil saturation was calculated.

(5) Aging was conducted in the 80 °C oven for 3 days to ensure full contact between the core and the crude oil.

(6) Backpressure was adjusted with a hand pump to the required pressure (8–24 MPa) and was stabilized.

(7) The pressure of the CO_2 container was maintained with an ISCO pump at slightly above or equal to the required displacement pressure. The inlet and outlet valves of the core holder were opened to start the displacement test.

(8) Injection pressure at the core inlet, produced oil volume, and produced gas volume at the outlet were recorded every minute. The total injected CO_2 was set to 1.6 PV, and the final CO_2 displacement recovery was calculated.

(9) The core was replaced, and steps (1) to (8) were repeated to obtain CO_2 displacement recovery at different displacement pressures.

(10) A plot of CO_2 displacement pressure versus oil recovery was constructed. The pressure corresponding to the inflection point of the curve was taken as the minimum miscible pressure (MMP) (Li et al., 2015, 2022). Compared with the traditional slim-tube method, this method featured a shorter experimental cycle and higher repeatability (Song et al., 2024; Yellig and Metcalfe, 1980).

2.3. Experimental method for evaluating core CO_2 displacement with MEAs

The CO_2 displacement method in Section 2.2 was used. All other steps were identical. Before step (7), 0.02 PV of different types of MEAs (i.e., petroleum ether, Tween 80, tributyl citrate, and lauryl alcohol polyether-4) were injected into the core. Immediately afterward, 1.6 PV CO_2 was injected continuously to conduct oil displacement. Injection of the MEA as a slug prior to CO_2 was selected mainly for simplicity of oilfield operations.

2.4. Core nuclear magnetic resonance analysis method

A low-field nuclear magnetic resonance analyzer (SPEC-RC035, Beijing SPEC) was used to measure T_2 spectra of cores at different CO_2 displacement stages. The test stages mainly included the oil-saturated stage and the CO_2 displacement stage (including the MEA injection stage). Changes in T_2 spectra between stages were analyzed to assess, at the microscopic scale, the extent of CO_2 conformance in different pores and to examine the microscopic mechanism of miscibility enhancement. During T_2 testing, pulse spacing (TAU) was 100 μs, sampling interval (DW) was 4 μs, number of scans (SCAN) was 32, and receiver gain (RG) was 20 dB.

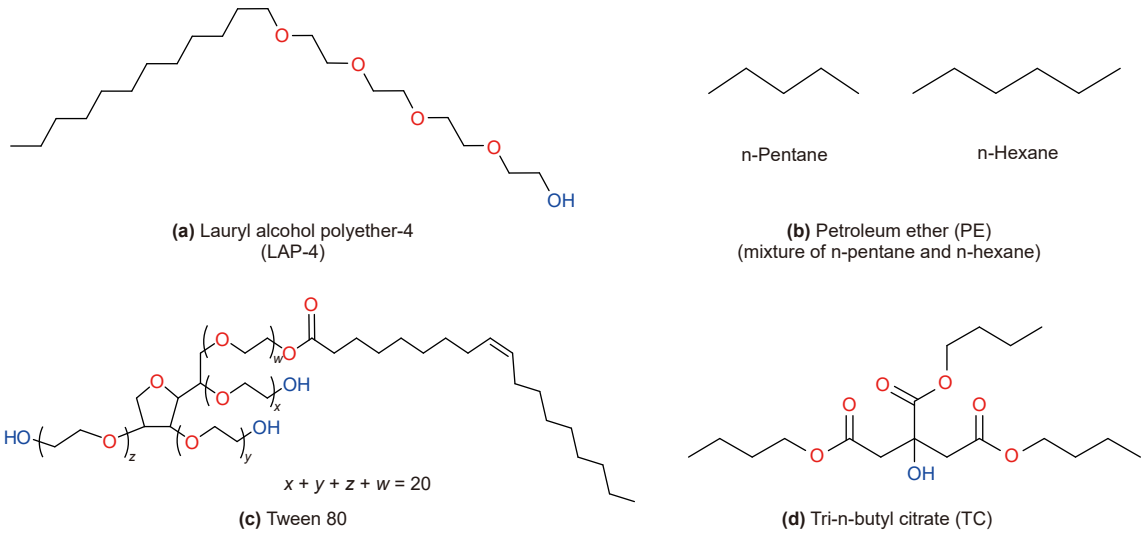

(a) Lauryl alcohol polyether-4 (LAP-4)

(b) Petroleum ether (PE) (mixture of n-pentane and n-hexane)

(c) Tween 80

(d) Tri-n-butyl citrate (TC)

Fig. 1. Chemical structures of different types of MEAs.

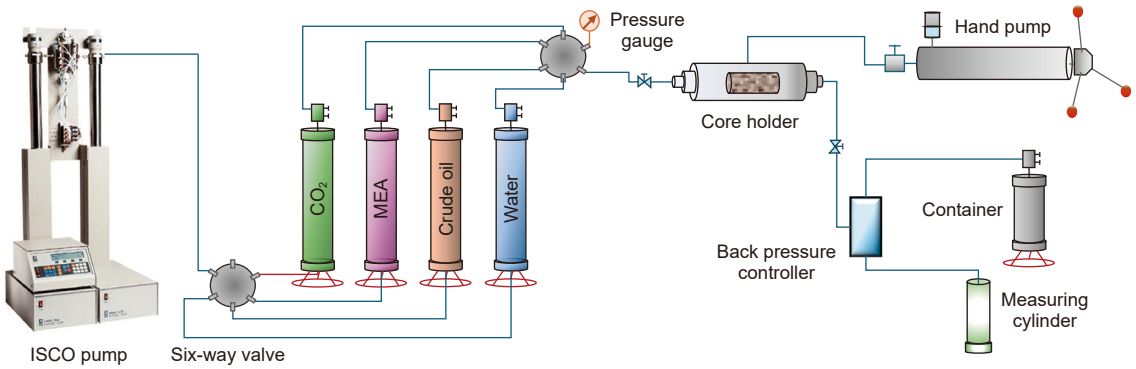

Fig. 2. Schematic diagram of core displacement test device.

3. Results and discussions

3.1. Measurement of CO_2–oil MMP in low-permeability reservoirs

Different experimental displacement pressures in the range of 8–24 MPa were set. A series of recovery factors under CO_2 displacement at these pressures was obtained. The reservoir pressure before CO_2 displacement process in the Xinjiang Oilfield was 18.7 MPa. The relationship between recovery factor and displacement pressure is shown in Fig. 3.

From Fig. 3, a turning point appeared between 20 and 22 MPa. Two fitted straight lines could be constructed. According to the principle of the core displacement method, the turning point was the minimum miscible pressure. Therefore, the MMP between the crude oil and CO_2 under these experimental conditions was 20.94 MPa. In addition, the reservoir pressure of the target formation for the CO_2 displacement pilot test was 18.7 MPa. At this pressure, the oil recovery under CO_2 displacement was only 70.4%. This value was 13.5 percentage points lower than at MMP. Therefore, screening of MEAs for CO_2 displacement was necessary.

3.2. Evaluation of CO_2 displacement performance with different MEAs

3.2.1. Analysis of displacement dynamics

The initial MEAs in this study were petroleum ether (PE), Tween 80, tributyl citrate (TC), and lauryl alcohol polyether-4 (LAP-4). Before CO_2 displacement, slugs of 0.02 PV of the above MEAs were injected. The experimental temperature was the reservoir temperature of 80 °C. The experimental pressure was 18.7 MPa, controlled by a backpressure device. For uniform comparison, the CO_2 injection volume during CO_2 displacement was set to 1.6 PV. The results were shown in Fig. 4.

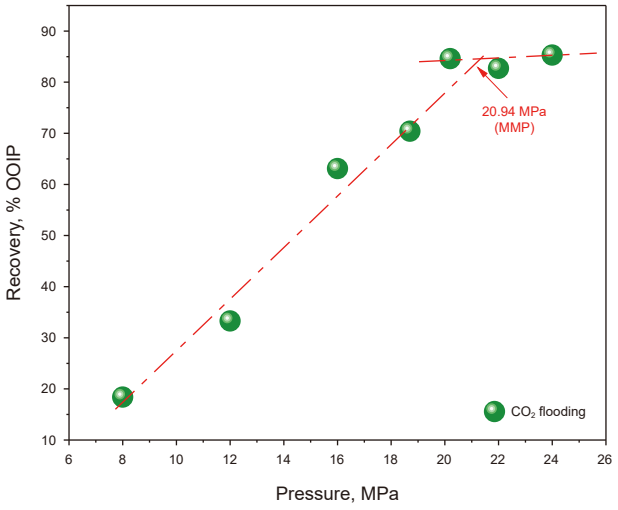

Fig. 3. Determination of MMP for CO_2 displacement without MEAs.

From Fig. 4(a), when no MEA was used, CO_2-only displacement did not reach the miscible pressure. The oil recovery was 70.4%. The oil recovery at (near) miscibility measured by the core displacement MMP method was 83.9%, which was 13.5 percentage points higher. Fig. 4(b)–(e) presents the displacement dynamics and recoveries after adding the four MEAs. With PE, Tween 80, LAP-4, and TC as MEAs, the recoveries at 18.7 MPa during subsequent CO_2 displacement were 80.8%, 82.7%, 84.6%, and 86.5%, respectively. Increases over the case without MEA were 10.4, 12.3, 14.2, and 16.1 percentage points, respectively. The highest recovery was obtained with tributyl citrate as the MEA. This recovery was 2.6 percentage points higher than the recovery at (near) miscibility (83.9%). Therefore, the use of TC as the MEA effectively increased miscibility between CO_2 and crude oil in porous media and improved oil recovery by CO_2 displacement.

3.2.2. Effect of MEAs on delaying CO_2 breakthrough

To further analyze the effect of MEAs, CO_2 displacement dynamics after MEA injection in Fig. 4 were used. In Fig. 5(a), CO_2 breakthrough times after different MEAs were compared. The outlet pressure of the core was maintained at 18.7 MPa to simulate reservoir pressure conditions. Relative to the case without MEA, CO_2 breakthrough was significantly delayed by all MEA injection. The effective CO_2 displacement time was extended.

The longest delay was obtained with tributyl citrate (TC). The order from high to low was Tween 80, PE, and LAP-4. Except for LAP-4, the delay in breakthrough time showed a strong correlation with oil recovery. Therefore, delaying breakthrough time was the first mechanism by which MEAs enhanced miscibility between CO_2 and crude oil. The main reason was that the delayed CO_2 breakthrough could increase mass transfer time between high-pressure CO_2 and crude oil. The miscibility interaction lasted longer, and thus more oil was displaced. Because of page-length limitations, quantitative investigation of the effects of different types of MEAs on oil recovery and gas channeling remained for subsequent, more in-depth study (He et al., 2025). The optimal MEA was selected only through core displacement experiments in this study.

3.2.3. Analysis of the effect of MEAs on CO_2 displacement pressure difference

Fig. 5(b) shows the displacement pressure difference during CO_2 displacement after MEA addition. Except for the case with

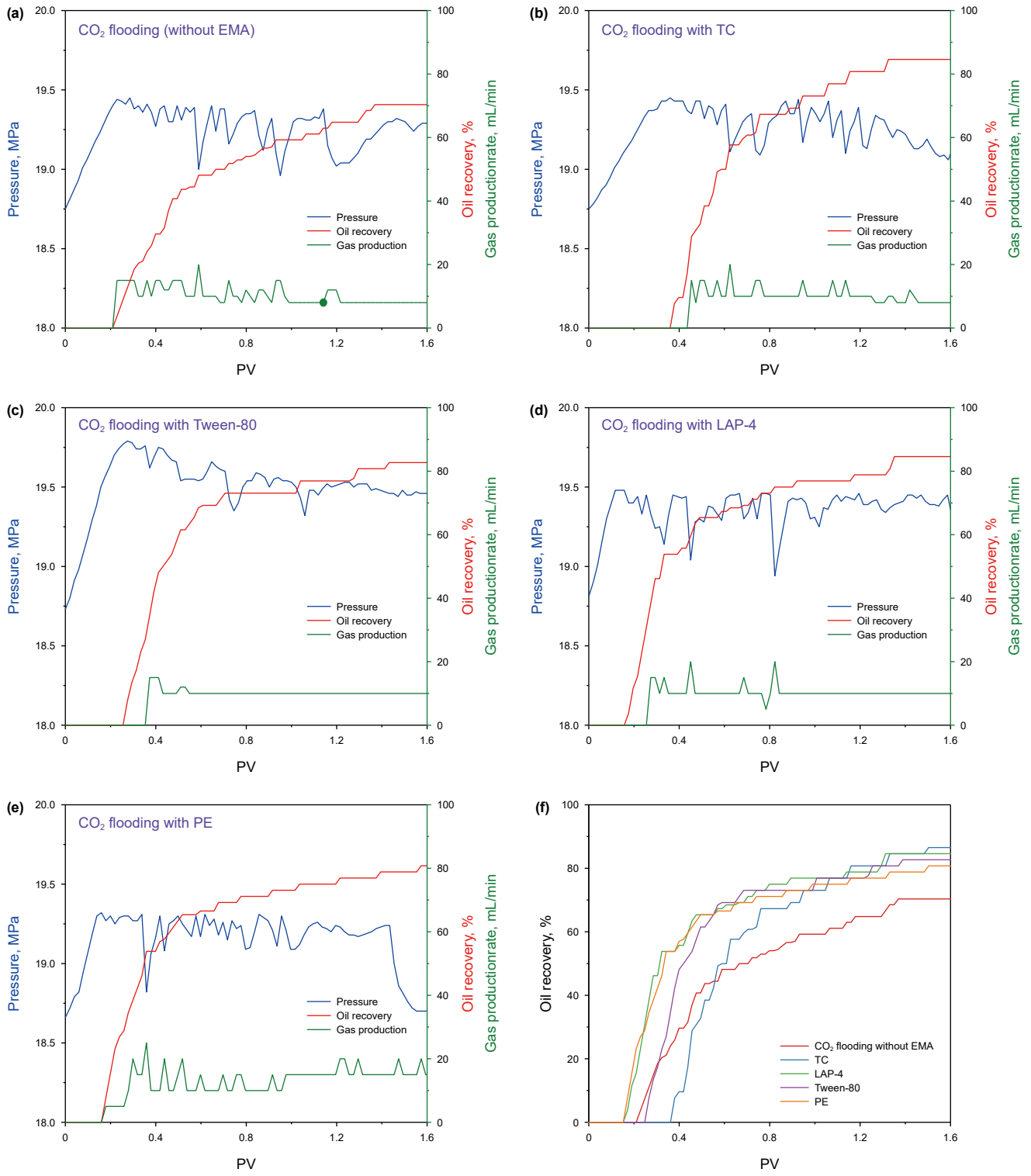

Fig. 4. Dynamic CO_2 displacement plots with different MEAs. (**a**) No MEA, (**b**)TC, (**c**) Tween 80, (**d**) LAP-4, (**e**) PE, (**f**) comparison of oil recovery with different MEAs.

Tween 80, the displacement pressure after adding MEAs changed little relative to CO_2 displacement without MEA. The displacement pressure with Tween 80 increased markedly. The main reason was the relatively high viscosity of Tween 80. The displacement pressure difference with LAP-4 and PE became smaller. The main reason was their strong solubility with crude oil. The relationship between injection pressure difference and oil recovery was weak. For MEAs such as Tween 80, increasing the CO_2 displacement pressure difference also enhanced miscibility between CO_2 and crude oil. As shown in Fig. 4, the addition of Tween 80 increased oil recovery by 12.3 percentage points. Therefore, increasing the CO_2 displacement pressure difference was the second mechanism by which MEAs enhanced miscibility between CO_2 and crude oil.

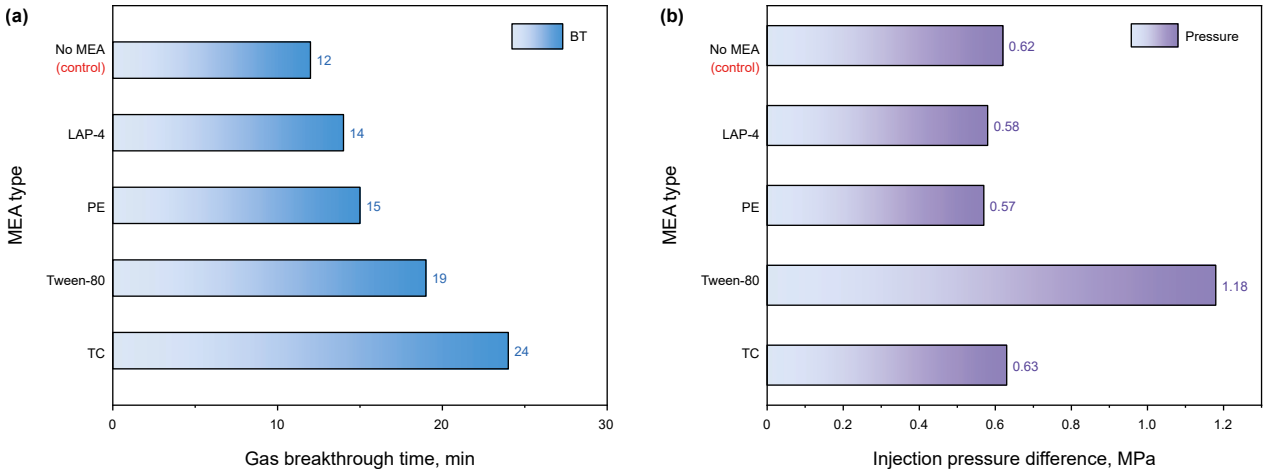

Fig. 5. Comparison of CO_2 displacement breakthrough time and pressure difference with different MEAs. (**a**) Breakthrough time; (**b**) displacement pressure difference.

3.3. Microscopic mechanism analysis of CO_2 displacement with MEAs based on NMR

To analyze the effect of different MEAs on improving oil recovery during CO_2 displacement and to further reveal their mechanism, a low-field NMR instrument was used. NMR T_2 spectra were measured for core samples saturated with water, saturated with oil, and after CO_2 displacement with MEAs. The experimental results are shown in Table 3. By analyzing changes in the peak areas of small and large pores and the cumulative signal amplitude in the T_2 spectra, the microscopic action mechanisms of MEAs were analyzed. Fig. 6 compares the NMR T_2 spectra at the end of CO_2 displacement with different types of MEAs.

From Fig. 6 and Table 3, after oil saturation, clear fluid signals were present in both small and large pores in the core. The peak with a relaxation time of 0–10 ms corresponded to small pores. The peak with a relaxation time of 10–1000 ms corresponded to large pores.

Compared with single CO_2 displacement, the change amplitude of the large-pore peak area in the core increased after displacement with added MEAs. The largest change rate was obtained with TC, at 95.71%. In addition, without MEA, CO_2 displacement displaced 91.17% of the oil in large pores, leaving 8.83% residual oil in large pores. Moreover, the oil in small pores increased under the action of CO_2. The main reason was that the oil in large pores dissolved in CO_2 and was pushed into small pores under pressure differential, which led to an increase of oil in small pores. Therefore, before the MMP was reached, CO_2 largely displaced oil in large pores, but the oil in small pores was almost not mobilized, and it could even increase. After adding MEAs (except PE), the oil in both large pores and small pores was mobilized to a great extent. The change rates of small-pore peak areas also increased markedly, except for PE. The largest increase was obtained with TC, at 18.97%. The magnitude of the change rate directly reflected the efficiency of oil displacement from pores of that size. Therefore, the addition of MEAs allowed CO_2 to contact more oil in small pores and displace it. This was the third mechanism of MEAs.

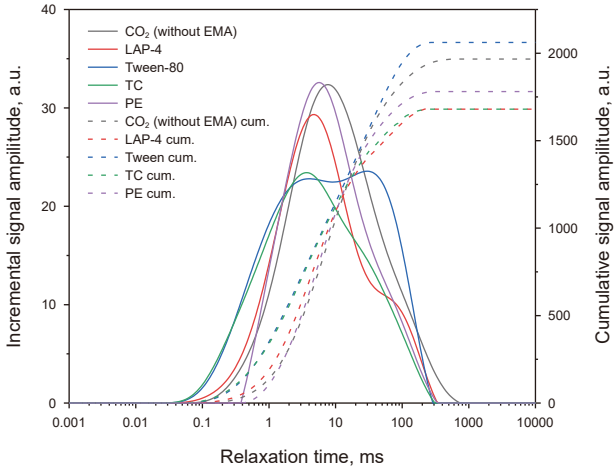

Fig. 6. NMR T_2 curves after displacement with different MEAs at 18.7 MPa.

Compared with other MEAs, displacement with TC yielded the largest change rates of NMR signal amplitudes in both small and large pores, and the highest oil recovery (86.5%, Fig. 4). Therefore, by integrating the core displacement results and the microscopic pore mobilization effect, TC was selected as the optimal MEA.

Table 3
Change rates of NMR T_2 peak areas during displacement with different agents.

Core No.	MEA type	Peak areas in the oil saturation stage, a.u.			Peak areas in the CO_2 displacement stage, a.u.			Change rates, %		
		10 ms$^-$	10 ms$^+$	Total	10 ms$^-$	10 ms$^+$	Total	10 ms$^-$	10 ms$^+$	Total
50-15	/	250	37,738	37,988	262	3332	3594	−4.80	91.17	90.54
50-13	LAP-4	266	35,227	35,493	245	1965	2210	7.89	94.42	93.77
50-7	Tween-80	242	37,417	37,659	212	3009	3221	12.40	91.96	91.45
50-16	TC	253	37,108	37,361	205	1591	1796	18.97	95.71	95.19
50-14	PE	244	31,219	31,463	270	1936	2206	−10.66	93.80	92.99

3.4. Effect of TC on reducing the MMP

To further determine the MMP between CO_2 and crude oil reduced by TC, core CO_2 displacement experiments were conducted at the same pressure points as in Fig. 4. The gas-measured permeability of the core was 50×10^{-3} μm^2, and the experimental temperature was 80 °C, to simulate the target reservoir conditions. A series of oil recovery data with TC was obtained, and a relationship curve between oil recovery and displacement pressure was plotted, as shown in Fig. 7.

After adding TC as a MEA, an inflection point appeared between 18.7 and 20 MPa in the relationship curve between oil recovery and experimental displacement pressure. Under these experimental conditions, the MMP between crude oil and CO_2 after adding TC was measured by core displacement to be 19.03 MPa, with a reduction of 1.91 MPa. Thus, miscibility between CO_2 and crude oil was significantly improved by adding TC. More contact between crude oil and CO_2 was achieved, and more crude oil was displaced.

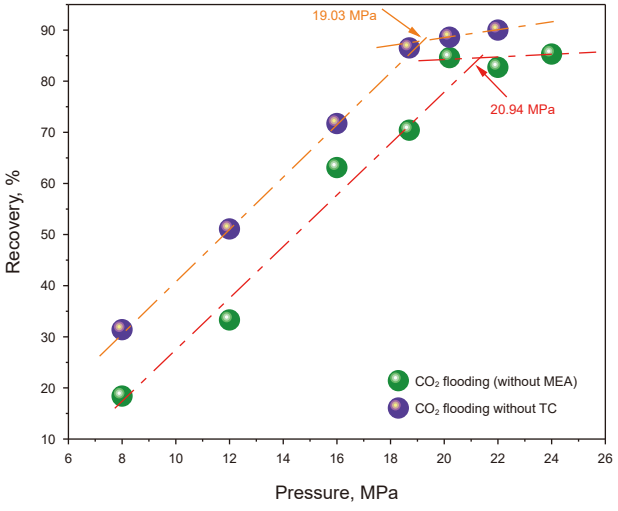

Fig. 7. Minimum miscible pressure of the CO_2–crude oil system after adding tributyl citrate.

Fig. 8 presented the gas channeling time and the injection pressure difference at different pressures when TC was used as an MEA. Compared with CO_2 displacement without the MEA, CO_2 displacement with TC significantly delayed the gas channeling time. When the displacement pressure was 18.7 MPa, the gas channeling time was extended by 12 min to 24 min. In addition, after adding TC, the pressure difference of CO_2 displacement slightly changed. Therefore, by delaying gas channeling, the mass transfer time between CO_2 and crude oil was increased, and more crude oil was displaced.

3.5. Microscopic mechanism analysis of TC increasing miscibility during CO_2 displacement based on NMR technique

Core samples after CO_2 displacement under different pressures with tributyl citrate added as a MEA were scanned by an NMR analyzer. Changes in peak areas of small and large pores and cumulative signal amplitudes on the T_2 spectra were observed. Fig. 9 shows the T_2 spectra after CO_2 gas displacement with TC under different pressures. Table 4 lists the change rates of peak areas in small and large pores.

From Fig. 9, two distinct peaks were observed in the core. The peak with relaxation time of 0–10 ms corresponded to small pores. The peak with relaxation time of 10–1000 ms corresponded to large pores. After adding the MEA and performing CO_2 displacement, the signal from large pores in the core decreased markedly. Since crude oil in large pores had good mobility, under the driving of injected CO_2, it was preferentially displaced and flowed toward the outlet. Oil saturation in large pores dropped sharply, and the NMR T_2 signal amplitude corresponding to large pores decreased significantly. With increasing displacement pressure, the large-pore peak-area change rates were increased from 76.98% to 98.08%. The rate of signal decrease showed an increasing trend. However, with increasing displacement pressure, the signal in small pores first increased and then decreased, indicating that crude oil in small pores was gradually displaced.

By comparing Fig. 8(a) with the data in Tables 4 and it was seen that when near-supercritical CO_2 conditions were reached, the diffusion ability of CO_2 was limited, the gas channeling time was long, and the miscibility with crude oil was limited. The oil recovery was only 31.4%. When the CO_2 displacement pressure became higher and reached 16.2 MPa, the gas channeling time was

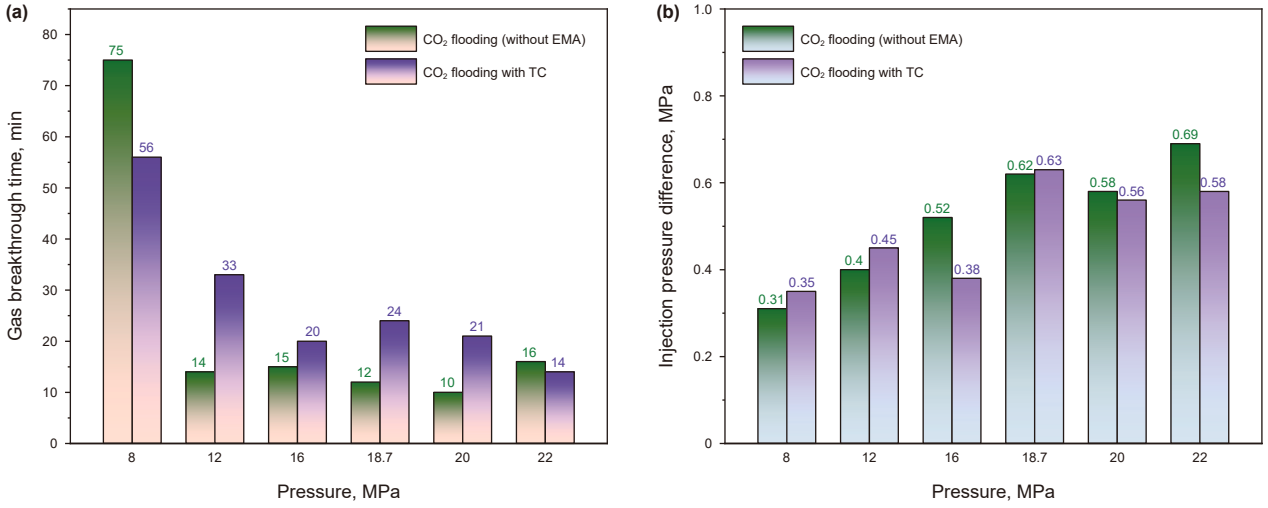

Fig. 8. Comparison of gas channeling time and pressure difference during CO_2 displacement with added tributyl citrate. (**a**) Gas channeling time; (**b**) displacement pressure difference.

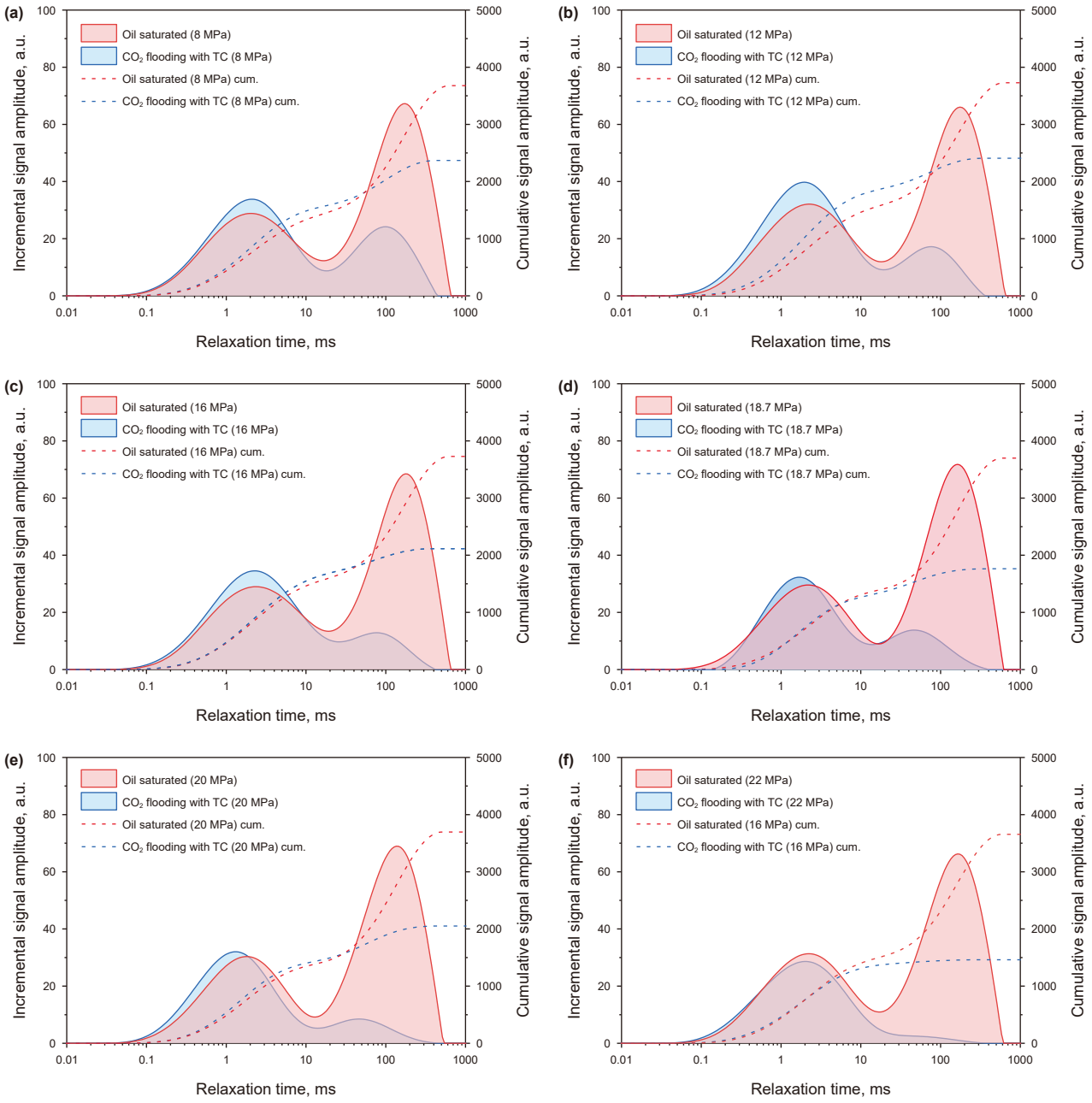

Fig. 9. NMR T_2 curves for CO_2 displacement with TC under different pressures. (**a**) 8 MPa, (**b**) 12 MPa, (**c**) 16 MPa, (**d**) 18.7 MPa, (**e**) 20 MPa, (**f**) 22 MPa.

Table 4
Peak-area change rates during TC-assisted displacement at different CO_2 flooding pressure.

Core No.	Pressure, MPa	Peak areas in the oil saturation stage, a.u.			Peak areas in the CO_2 displacement stage, a.u.			Change rates, %		
		10 ms$^-$	10 ms$^+$	Total	10 ms$^-$	10 ms$^+$	Total	10 ms$^-$	10 ms$^+$	Total
50-25	8	214	24,462	24,676	231	5632	5863	−7.94	76.98	76.24
50-37	12	240	23,801	24,041	266	3054	3320	−10.83	87.17	86.19
50-29	16	231	24,908	25,139	257	2583	2840	−11.26	89.63	88.70
50-21	18.7	212	24,485	24,697	189	1956	2145	10.85	92.01	91.31
50-27	20	194	20,428	20,622	162	1187	1349	16.49	94.19	93.46
50-38	22	228	22,550	22,778	196	433	629	14.03	98.08	97.24

shortened significantly. It was mainly because under supercritical and near-miscible conditions, the diffusion ability of CO_2 in crude oil became stronger. At 20 MPa (near the MMP obtained by the core displacement method), the NMR T_2 signal from small pores was minimal, indicating that CO_2 displaced most of the crude oil in small pores at that time. By combining the results in Fig. 8 and

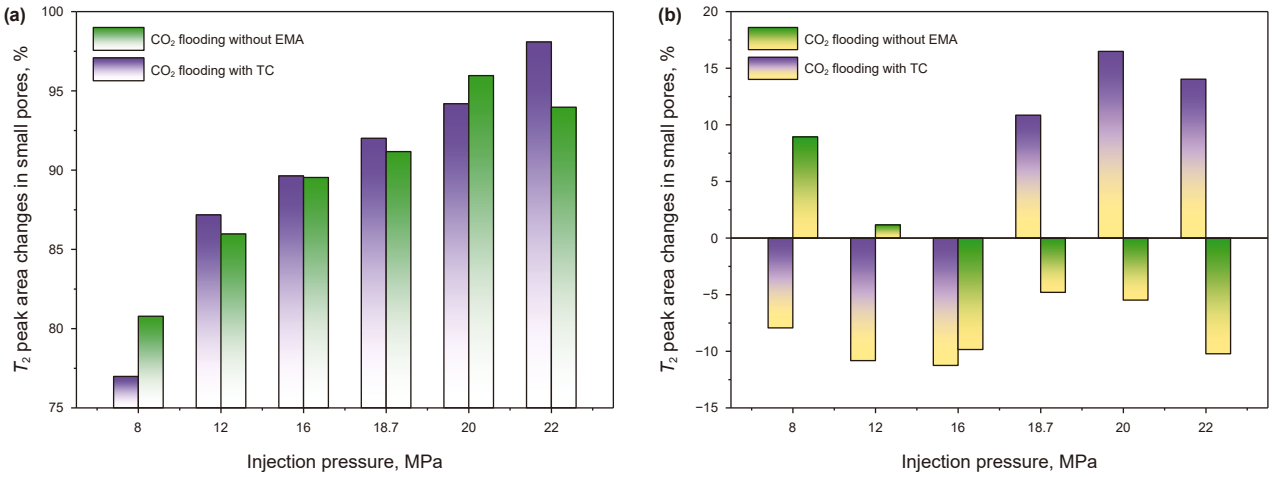

Fig. 10. Comparison of NMR T_2 spectral peak areas during CO_2 displacement before and after adding TC as EMA. (**a**) Large pores; (**b**) small pores.

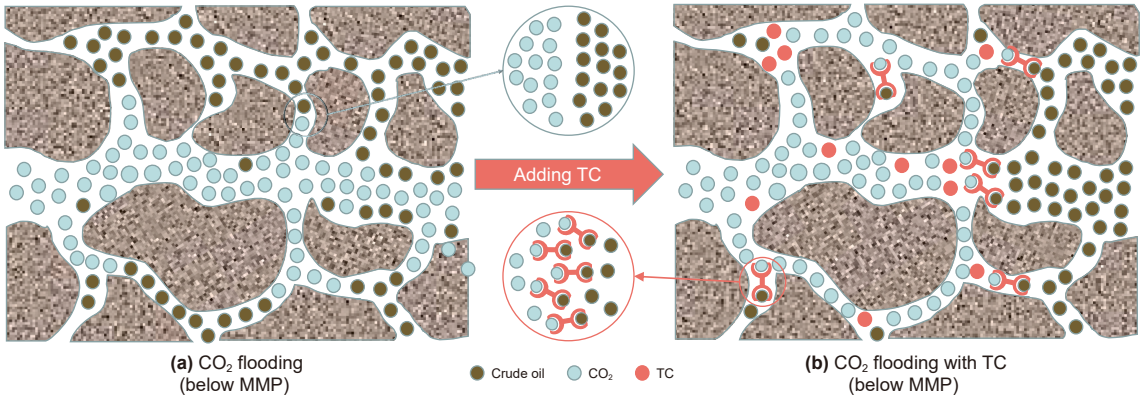

Fig. 11. Schematic of the miscibility-enhancing mechanism of TC as a miscibility-enhancing agent.

Tables 4 and it was concluded that under reservoir pressure (i.e., 18.7 MPa), when TC was added as a MEA, appropriate gas channeling and displacement pressure were present, which led to high CO_2 displacement recovery.

Fig. 10 presented a comparison of the peak areas of large- and small-pore signals on NMR T_2 spectra during CO_2 displacement before and after addition of the MEA. After TC was added, decreases in large-pore signals in the core were observed during CO_2 displacement. The rate of signal change increased as displacement pressure increased. Thus, with increasing displacement pressure, CO_2 displacement after injection of TC effectively increased the miscibility between CO_2 and crude oil in large pores and increased oil recovery. When the displacement pressure approached the MMP, CO_2 displacement after adding TC effectively increased the miscibility between CO_2 and crude oil in the core's small pores. Oil saturation in small pores was significantly reduced, and the corresponding NMR signal of small pores decreased.

Fig. 11 presents the mechanism by which TC enhanced CO_2–oil miscibility. The effect was mainly attributed to delayed gas channeling and diffusion into small pores, by which more oil was displaced. Molecular-level interactions were proposed to require further study using molecular simulation.

Of course, unconventional oil and gas reservoirs such as shale reservoirs still existed. During development, hydraulic fracturing was usually used and dense fracture networks were generated. Analysis of the effectiveness of MEA in low-permeability reservoirs with fractures remained to be investigated in subsequent studies. The modes of reducing MMP under fracture-matrix dual-media conditions and the influence of reservoir facies on MEA effectiveness also remained to be investigated. In addition, CO_2 reacted with shale and carbonate reservoir rocks. When NMR was applied to those reservoirs, the effect of changes in the pore-network structure needed to be considered. The cores in this study were sandstone samples. Changes in the pore network during CO_2 displacement could be neglected. Further study was warranted regarding the effects of MEA on rock pore-throat geometry and on the microscale mechanisms of fluid–rock interactions. Finally, further study was required on the potential environmental and operational implications of MEA, if the agent was selected for large-scale oilfield applications.

4. Conclusions

This study was based on the established displacement experiment for determining the MMP of CO_2 displacement. Suitable MEAs were screened. The miscibility-enhancing mechanism of the MEA was analyzed with NMR. The following main results were obtained.

(1) A method based on core displacement experiments was established to determine the MMP of CO_2 displacement. The MMP between CO_2 and the crude oil was measured as 20.94 MPa.

(2) Compared with CO_2 displacement without MEA, oil recovery during CO_2 displacement after adding different MEAs was significantly increased. Lauryl alcohol polyether-4 (LAP-4) and tributyl citrate (TC) showed better recovery improvement, with increases exceeding 20%.
(3) After adding four different MEAs, gas channeling time was delayed. TC showed the best delay, with gas channeling time reaching 24 min.
(4) By the core displacement method, after adding TC, the MMP was reduced from 20.94 to 19.03 MPa. A significant enhancement of CO_2–oil miscibility was indicated.
(5) After adding TC during CO_2 displacement, NMR T_2 spectra showed decreases in large-pore signals in the core. The magnitude of the signal decrease increased with displacement pressure. An effective increase in conformance in large pores within preferential channels was indicated.
(6) When displacement pressure approached the MMP, CO_2 entered small pores, but oil droplets were not effectively displaced and remained trapped. After adding TC, microscopic conformance in small pores was increased.
(7) Enhancement of CO_2–oil miscibility by TC was mainly attributed to delayed gas channeling time and diffusion into small pores, which displaced more oil.
(8) An implementable chemical scheme to enhance CO_2-EOR performance in the CCUS pilot in the XinJiang Oilfield was provided. A reference for other similar reservoirs was also provided.
(9) This study was mainly experimental and further research was required on the molecular interaction mechanisms among MEA, CO_2, and crude oil, and on potential environmental issues.

Funding

This work was supported by the Oil & Gas Major Project (2025ZD1405006) and Natural Science Foundation of Xinjiang Uygur Autonomous Region (No. 2022D01A250).

CRediT authorship contribution statement

Chuan-Jie Ren: Writing – original draft, Validation, Investigation. **Yong-Liang Yang:** Writing – original draft, Visualization, Validation, Investigation, Data curation. **Hong-Jun Zhang:** Validation, Investigation, Data curation. **Dao-Yi Zhu:** Writing – review & editing, Validation, Supervision, Project administration, Investigation, Data curation.

Declaration of competing interest

The authors declare that they have no known competing financial interests or personal relationships that could have appeared to influence the work reported in this paper.

References

Al-Hakami, M.A., Ibrahim, A.F., Abdelgawad, K.Z., 2025a. Applications of ionic liquids in improving CO_2 miscibility in crude oil for enhanced oil recovery and CO_2 sequestration applications. J. Supercrit. Fluids 219, 106539. https://doi.org/10.1016/j.supflu.2025.106539.

Al-Hakami, M.-A., Ibrahim, A.-F., Abdelgawad, K.-Z., et al., 2025b. Improving CO_2 miscibility in crude oil utilizing viscosity reducer: experimental and molecular simulation study. Arabian J. Sci. Eng. 50 (24), 21455–21467. https://doi.org/10.1007/s13369-025-10417-1.

Almobarak, M., Wu, Z., Zhou, D., et al., 2021. A review of chemical-assisted minimum miscibility pressure reduction in CO_2 injection for enhanced oil recovery. Petroleum 7 (3), 245–253. https://doi.org/10.1016/j.petlm.2021.01.001.

Bai, L., Gao, Y., Yang, S., et al., 2025. Nanosheet-reinforced CO_2 foam systems for CO_2 conformance control: Effects of reservoir permeability and heterogeneity. Energy Fuels. 39 (37), 17834–17844. https://doi.org/10.1021/acs.energyfuels.5c03934.

Cao, M., Gu, Y., 2013a. Oil recovery mechanisms and asphaltene precipitation phenomenon in immiscible and miscible CO_2 flooding processes. Fuel 109, 157–166. https://doi.org/10.1016/j.fuel.2013.01.018.

Cao, M., Gu, Y., 2013b. Physicochemical characterization of produced oils and gases in immiscible and miscible CO_2 flooding processes. Energy Fuels. 27 (1), 440–453. https://doi.org/10.1021/ef301407k.

Costa Gomes, M.-F., Pádua, A.-A., 2003. Interactions of carbon dioxide with liquid fluorocarbons. J. Phys. Chem. B 107 (50), 14020–14024. https://doi.org/10.1021/jp0356564.

Du, L., Kelly, J.-Y., Roberts, G.-W., et al., 2009. Fluoropolymer synthesis in supercritical carbon dioxide. J. Supercrit. Fluids 47 (3), 447–457. https://doi.org/10.1016/j.supflu.2008.11.011.

Eastoe, J., Dupont, A., Steytler, D.C., 2003. Fluorinated surfactants in supercritical CO_2. Curr. Opin. Colloid Interface Sci. 8 (3), 267–273. https://doi.org/10.1016/S1359-0294(03)00053-0.

Enick, R., Beckman, E., Yazadi, A., et al., 1998. Phase behavior of CO_2–perfluoropolyether oil mixtures and CO_2–perfluoropolyether chelating agent mixtures. J. Supercrit. Fluids 13 (1–3), 121–126. https://doi.org/10.1016/S0896-8446(98)00043-6.

Fu, G.-T., Zheng, Z.-G., Zhang, Y.-Q., et al., 2024. High-pressure CO_2 solubility in crude oil and CO_2 miscibility effects on oil recovery performance in low-permeability reservoirs. Energy Fuels. 38 (24), 23433–23446. https://doi.org/10.1021/acs.energyfuels.4c05040.

Gandomkar, A., Torabi, F., Nasriani, H.R., et al., 2025. Maximising CO_2 sequestration efficiency in deep saline aquifers through in-situ generation of CO_2-in-brine foam incorporating novel CO_2-soluble non-ionic surfactants. Chem. Eng. J., 166102 https://doi.org/10.1016/j.cej.2025.166102.

Gao, P., Towler, B., Pan, G., 2010. Strategies for evaluation of the CO_2 miscible flooding process. In: Abu Dhabi International Petroleum Exhibition and Conference. SPE-138786-MS. https://doi.org/10.2118/138786-MS.

Guan, J., Li, S., Li, Z., 2025. Chemical strategies for enhancing CO_2 underground storage and oil recovery efficiency: A comprehensive review and future perspectives. Chem. Eng. J., 169092 https://doi.org/10.1016/j.cej.2025.169092.

Guo, P., Hu, Y.S., Qin, J.S., et al., 2017. Use of oil-soluble surfactant to reduce minimum miscibility pressure. Petrol. Sci. Technol. 35 (4), 345–350. https://doi.org/10.1080/10916466.2016.1259630.

He, X., Zhang, K., Jiang, S., et al., 2025. Influencing factors and quantitative prediction of gas content of deep marine shale in Luzhou block. Sci. Rep. 15 (1), 1896. https://doi.org/10.1038/s41598-025-86095-8.

Kuang, N., Yang, S., Yuan, Z., et al., 2021. Study on oil and gas amphiphilic surfactants promoting the miscibility of CO_2 and crude oil. ACS Omega 6 (41), 27170–27182. https://doi.org/10.1021/acsomega.1c03822.

Li, M., Lim, V.-M., Ghafri, S.-Z., et al., 2022. Minimum miscibility pressure of CO_2 and oil evaluated using MRI and NMR measurements. J. Petrol. Sci. Eng. 214, 110515. https://doi.org/10.1016/j.petrol.2022.110515.

Li, F.F., Yang, S.L., Chen, H., et al., 2015. An improved method to study CO_2–oil relative permeability under miscible conditions. J. Pet. Explor. Prod. Technol. 5 (1), 45–53. https://doi.org/10.1007/s13202-014-0122-1.

Li, S., Zhu, J., Wang, Z., et al., 2024. Chemical strategies for enhancing CO_2-Hydrocarbon miscibility. Separ. Purif. Technol. 337, 126436. https://doi.org/10.1016/j.seppur.2024.126436.

Liu, S.Y., Li, M.F., Chen, J.Y., et al., 2025. Experimental investigation of surfactants and their ethanol blends for CO_2–oil miscibility enhancement in CO_2-EOR. Pet. Sci. 22 (10), 4271–4281. https://doi.org/10.1016/j.petsci.2025.07.005.

Liu, J., Sun, L., Li, Z., et al., 2019. Experimental study on reducing CO_2–oil minimum miscibility pressure with hydrocarbon agents. Energies 12 (10), 1975. https://doi.org/10.3390/en12101975.

Luo, Y., Yang, S., Zhang, Y., et al., 2024. Characteristics and mechanisms of CO_2 flooding with varying degrees of miscibility in reservoirs composed of low-permeability conglomerate formations. Processes 12 (6), 1203. https://doi.org/10.3390/pr12061203.

Sarbu, T., Styranec, T., Beckman, E.-J., 2000. Non-fluorous polymers with very high solubility in supercritical CO_2 down to low pressures. Nature 405 (6783), 165–168. https://doi.org/10.1038/35012040.

Sennaoui, B., Pu, H., Afari, S., et al., 2022. Pore-and core-scale mechanisms controlling supercritical cyclic gas utilization for enhanced recovery under immiscible and miscible conditions in the three forks formation. Energy Fuels. 37 (1), 459–476. https://doi.org/10.1021/acs.energyfuels.2c02938.

Song, G., Meng, Y., Zhang, C., et al., 2024. Comprehensive review of the determination and reduction of the minimum miscibility pressure during CO_2 flooding. ACS Omega 9 (13), 14747–14765. https://doi.org/10.1021/acsomega.4c00469.

Song, Y., Zhang, Q., Zou, X., et al., 2025. Research progress on and outlook of direct CO_2 thickeners for enhanced oil recovery. RSC Adv. 15 (2), 714–731. https://doi.org/10.1039/D4RA07300B.

Voon, C., Awang, M., 2014. Reduction of MMP using oleophilic chemicals. Int. J. Chem., Mol., Nuclear Ma. Metallurgical Engi. 8 (4), 351–353. https://doi.org/10.5281/ZENODO.1094316.

Wang, X., Gu, Y., 2011. Oil recovery and permeability reduction of a tight sandstone reservoir in immiscible and miscible CO_2 flooding processes. Ind. Eng. Chem. Res. 50 (4), 2388–2399. https://doi.org/10.1021/ie1016046.

Wang, Z.G., Huang, H., Chen, H.Y., et al., 2024. Research progress on reducing the minimum miscibility pressure of CO_2 flooding. In: International Field

Exploration and Development Conference. Springer, pp. 931–942. https://doi.org/10.1007/978-981-96-5226-6_67.
Wang, Z., Zhu, J., Li, S., 2023. Novel strategy for reducing the minimum miscible pressure in a CO_2–oil system using nonionic surfactant: insights from molecular dynamics simulations. Appl. Energy 352, 121966. https://doi.org/10.1016/j.apenergy.2023.121966.
Yang, Z., Wu, W., Dong, Z., et al., 2019. Reducing the minimum miscibility pressure of CO_2 and crude oil using alcohols. Colloids Surf. A Physicochem. Eng. Asp. 568, 105–112. https://doi.org/10.1016/j.colsurfa.2019.02.004.
Yellig, W., Metcalfe, R., 1980. Determination and prediction of CO_2 minimum miscibility pressures (includes associated paper 8876). J. Petrol. Technol. 32 (1), 160–168. https://doi.org/10.2118/7477-PA.
Zhao, M., Xie, Y., Meng, X., et al., 2025a. Enhanced oil recovery through CO_2 injection: The role of pentane in improving miscibility of CO_2 and oil. Fuel 392, 134935. https://doi.org/10.1016/j.fuel.2025.134935.
Zhao, S., Liu, L., Li, Z., et al., 2025b. Experimental Study on the optimization of CO_2 flooding miscibility-reducing agents for low permeability reservoirs. ACS Omega 10 (14), 14362–14372. https://doi.org/10.1021/acsomega.5c00579.
Zhao, Y., Fan, G., Song, K., et al., 2021. The experimental research for reducing the minimum miscibility pressure of carbon dioxide miscible flooding. Renew. Sustain. Energy Rev. 145, 111091. https://doi.org/10.1016/j.rser.2021.111091.
Zhou, D., Lian, L., Wu, Z., et al., 2022. Optimization Design and Evaluation of Improved Miscible Assistants for CO_2 Flooding and the Application in Pilot in L Reservoir. International Petroleum Technology Conference. 21–23 February, Riyadh, Saudi Arabia. https://doi.org/10.2523/IPTC-22244-MS.
Zhu, D., 2022. CO_2 and GeoEnergy Engineering, China Petrochemical Press, Beijing (in Chinese).
Zhu, D., 2025. New Advances in Low-Energy Processes for Geo-Energy Development. Energies 18 (9), 2357. https://doi.org/10.3390/en18092357.
Zhu, D., Yang, Y., Tan, H., et al., 2026. CO_2 conformance control and carbon storage performance of particle gels in fractured reservoirs using nuclear magnetic resonance methods. SPE J. 31 (1), 588–601. https://doi.org/10.2118/231408-PA.